Glycobiology vol. 17 no. 1 pp. 104–118, 2006
doi:10.1093/glycob/cwl057
Advance Access publication on September 29, 2006

Comparison of biological activity among nonfucosylated therapeutic IgG1 antibodies with three different *N*-linked Fc oligosaccharides: the high-mannose, hybrid, and complex types

Yutaka Kanda, Tsuyoshi Yamada, Katsuhiro Mori, Akira Okazaki, Miho Inoue, Kazuko Kitajima-Miyama, Reiko Kuni-Kamochi, Ryosuke Nakano, Keiichi Yano, Shingo Kakita, Kenya Shitara, and Mitsuo Satoh[1]

Tokyo Research Laboratories, Kyowa Hakko Kogyo Co., Ltd, 3-6-6 Asahi-machi, Machida-shi, Tokyo 194-8533, Japan

Received on August 23, 2006; revised on September 25, 2006; accepted on September 25, 2006

The structure of asparagine-linked oligosaccharides attached to the antibody constant region (Fc) of human immunoglobulin G1 (IgG1) has been shown to affect the pharmacokinetics and antibody effector functions of antibody-dependent cellular cytotoxicity (ADCC) and complement-dependent cytotoxicity (CDC). However, it is still unclear how differences in the *N*-linked oligosaccharide structures impact the biological activities of antibodies, especially those lacking core fucose. Here, we succeeded in generating core fucose-lacking human IgG1 antibodies with three different *N*-linked Fc oligosaccharides, namely, a high-mannose, hybrid, and complex type, using the same producing clone, and compared their activities. Cultivation of an α-1,6-fucosyltransferase (*FUT8*) knockout Chinese hamster ovary cell line in the presence or absence of a glycosidase inhibitor (either swainsonine or kifunensine) yielded antibody production of each of the three types without contamination by the others. Two of three types of nonnaturally occurring atypical oligosaccharide IgG1, except the complex type, reduced the affinity for both human lymphocyte receptor IIIa (FcγRIIIa) and the C1q component of the complement, resulting in reduction of ADCC and CDC. The bulky structure of the nonreducing end of *N*-linked Fc oligosaccharides is considered to contribute the CDC change, whereas the structural change in the reducing end, i.e. the removal of core fucose, causes ADCC enhancement through improved FcγRIIIa binding. In the pharmacokinetic profile, although no significant difference of human neonatal Fc receptor (FcRn)-binding affinity was observed among the three types, the complex type showed longer serum half-lives than the other types irrespective of core fucosylation in mice, which also suggests the contribution of the nonreducing end structure. The present study provides basic information on the effects of core fucose-lacking *N*-linked Fc oligosaccharides on antibody biological activities.

[1]To whom correspondence should be addressed; Tel: +81 42-725-2556; Fax: +81 42-726-8330; e-mail: msatoh@kyowa.co.jp

Keywords: antibody effector functions/Fc oligosaccharides/IgG1 lacking core-fucosylation/*N*-linked oligosaccharide structure/pharmacokinetics

Introduction

The basic structure of a human immunoglobulin G1 (IgG1) molecule consists of two immunoglobulin light chains and two immunoglobulin heavy chains in covalent and noncovalent association to form three independent protein moieties connected through a flexible linker, designated as the hinge region. Two of these moieties, referred to as the Fab regions, are of identical structure, and each expresses a specific antigen-binding site. The third moiety, the antibody constant region (Fc), expresses antibody effector functions of antibody-dependent cellular cytotoxicity (ADCC) and complement-dependent cytotoxicity (CDC) through the interaction of the Fc either with lymphocyte receptors (FcγRs) on effector cells such as natural killer (NK) cells or with the C1q component of the complement (Jefferis et al. 1998; Jefferis and Lund 2002). The Fc is a homodimer comprising covalently disulfide-bonded hinge regions, the C_H2 domains glycosylated through covalent attachment of oligosaccharide at asparagine 297 and noncovalently paired C_H3 domains (Huber et al. 1976; Harris et al. 1998; Radaev et al. 2001). Human serum IgG is a glycoprotein with an average of 2.8 *N*-linked oligosaccharides per IgG molecule; the C_H2 domain of the Fc contains 2.0 of these *N*-linked oligosaccharides, whereas the hypervariable region of the Fab regions contains 0.8 (Mizuochi et al. 1982; Rademacher et al. 1988). Most of the therapeutic antibodies that are currently licensed and under development as medical agents are human IgG1s bearing two *N*-linked oligosaccharides bound to the Fc, because the oligosaccharides attached to the Fab regions are not necessary to achieve therapeutic antibody activity. The oligosaccharide attached to the Fc of human serum IgG1 as well as therapeutic antibodies is of the biantennary complex type and is composed of a mannosyl-chitobiose core structure in the presence or absence of a core fucose, a bisecting *N*-acetylglucosamine (GlcNAc), and terminal galactoses and sialic acids, giving rise to heterogeneities with a mixture of 30 or more glycoforms (Mizuochi et al. 1982; Harada et al. 1987; Rademacher et al. 1988; Schenerman et al. 1999; Jefferis 2002; Kamoda et al. 2004). Among these naturally occurring glycoforms, it has been shown that core fucosylation is the most important oligosaccharide structure affecting ADCC in vitro and in vivo, with the fucose residue attaching to the innermost GlcNAc of the *N*-linked biantennary complex-type Fc oligosaccharides (Shields et al. 2002;

Shinkawa et al. 2003; Niwa, Hatanaka et al. 2004; Niwa, Natsume et al. 2005; Niwa, Sakurada et al. 2005; Niwa, Shoji-Hosaka et al. 2004; Yamane-Ohnuki et al. 2004; Jefferis 2005; Iida et al. 2006).

The *N*-linked oligosaccharides have a basic common trimannosyl core structure composed of pentasaccharides, and they are classified into three types, namely, a high-mannose, hybrid, and complex type. The high-mannose type has oligosaccharide structures in which mannose alone binds to the nonreducing end of the core structure. The complex type has oligosaccharide structures in which the nonreducing end of the core structure has more than two GlcNAc's as well as a variable number of galactoses and sialic acids. The hybrid type has oligosaccharide structures in which the nonreducing end of the core structure has branches of both the high-mannose type and the complex type. In general, two broad classes of *N*-linked oligosaccharides, the complex type and the high-mannose type, can be attached to glycoproteins in mammals, depending on the protein. Neither the high-mannose type nor the hybrid type is a natural glycoform of the oligosaccharide attached to the Fc of human IgG1, although a minor population of the high-mannose type has been marginally detected in recombinant therapeutic antibodies produced in rodent mammalian cell lines such as Chinese hamster ovary (CHO) and mouse myeloma NS0 (Schenerman et al. 1999; Kamoda et al. 2004).

Several studies of biological activities with such nonnaturally occurring atypical oligosaccharide antibodies produced by mammalian cells have been reported. The specific inhibitors to α-1,2-glucosidase I of castanospermine and deoxynojirimycin have been used to probe the functional consequences of the high-mannose type Fc oligosaccharides of mouse IgG2a (the mouse counterpart of human IgG1) and IgG2b, and ADCC mediated by human NK cells has been shown to be enhanced by the glycoform alteration induced by these glucosidase inhibitors (Rothman et al. 1989; Awwad et al. 1990). A recombinant mouse/human chimeric IgG1 produced in a mutant CHO cell line Lec1, lacking *N*-acetylglucosaminlytransferase I (*GnT-I*), is reported to have the high-mannose type Fc oligosaccharides comprising a relatively small mannose moiety of 5 mannoses and to exhibit a slightly reduced affinity for human FcγRI, a severe deficiency in complement activation, and a reduced in vivo half-life time compared with the native IgG1 produced in parent CHO cells (Wright and Morrison 1994, 1998). The shortened serum half-life is revealed to be due to liver catabolism through mannose receptors (Wright et al. 2000). Inhibition of processing of *N*-linked oligosaccharides on mouse IgG2a by using swainsonine, which causes the structural change of the core-fucosylated oligosaccharides from complex type to hybrid type by α-mannosidase II inhibition, is reported to have no influence on antibody effector functions of CDC and ADCC mediated by mouse spleen cells (Nose and Heyman 1990). By contrast, the ADCC mediated by interferon-γ-activated human polymorphonuclear leukocytes is shown to be decreased by the core-fucosylated hybrid-type alteration induced by swainsonine (Rothman et al. 1989). Treating antibody-producing cells with monensin has firstly been reported to change the core-fucosylated complex-type Fc oligosaccharides to the hybrid-type-lacking core fucose, and the nonfucosylated hybrid-type mouse IgG2a is found to have enhanced ADCC through the FcγRIIIa on human NK cells (Rothman et al. 1989). Overexpression of β-1,4-*N*-acetylglucosaminyltransferase III (*GnT-III*) in antibody-producing cells has recently been shown to lead to enriched production of the bisected nonfucosylated hybrid-type antibodies, designated as Glyco-1 (Schuster et al. 2005; Ferrara, Brunker et al. 2006; Ferrara, Stuart et al. 2006). Glyco-1 humanized IgG1s are confirmed to feature increased ADCC through improved human FcγRIIIa binding and reduced CDC compared with the native unmodified IgG1s bearing the core-fucosylated complex type (Schuster et al. 2005; Ferrara, Brunker et al. 2006; Ferrara, Stuart et al. 2006). However, it is still unclear how these three basic structures of *N*-linked Fc oligosaccharides influence the biological activities of human IgG1 antibodies lacking core-fucosylation, because there has been no direct antibody activity comparison among the high-mannose-type, the hybrid-type, and the complex-type human IgG1s. In the present study, we succeeded in preparing these three different types of human IgG1s lacking the Fc core-fucosylation by using the same clone used to produce the recombinant anti-human CD20 mouse/human chimeric IgG1 rituximab and directly compared these biological antibody activities in side-by-side experiments.

Results

Generation of nonfucosylated IgG1 with three different Fc oligosaccharides

Monoclonal recombinant anti-human CD20 mouse/human chimeric IgG1, known as rituximab, was generated using CHO cell lines such as the α-1,6-fucosyltransferase (*FUT8*) knockout cell line Ms704, the guanosine diphosphate (GDP)-mannose 4,6-dehydratase (*GMD*)-deficient cell line Lec13, and the *GnT-I*-deficient cell line Lec1 as host cells. The products purified from each culture supernatant were confirmed by sodium dodecyl sulfate polyacrylamide electrophoresis (SDS–PAGE) to have an IgG1 structure identical to that of the control rituximab, without degradation or aggregation. The anti-human CD20s have an amino acid sequence equivalent to that of rituximab, which is widely used for the treatment of non-Hodgkin's lymphoma, and thus showed identical binding activity to the specific antigen in the antigen-binding enzyme-linked immunosorbent assay (ELISA) (Figure 1). Flow cytometric analysis also confirmed the identical antigen-binding activity irrespective of the Fc oligosaccharide structures (data not shown). Monosaccharide composition analysis confirmed that there was no fucose in the antihuman CD20s produced by clones from Ms704 and Lec1 (Table I). As expected, the oligosaccharide analysis clearly showed that antihuman CD20s bearing the three different types of *N*-linked Fc oligosaccharides were successfully generated by the combination of various CHO host cells with glycosidase inhibitors (Table II). Lec13 produced anti-human CD20 with core-fucosylated [Fu(+)] complex-type glycoforms comparable with rituximab when cultured in the medium containing L-fucose (Figure 2A and B). The Fc oligosaccharides of Ms704 producing antihuman CD20 were of the nonfucosylated [Fu(−)] complex type when cultured without glycosidase inhibitors (Figure 2C). Cultivation of either Ms704 or Lec13 with a specific inhibitor

of α-mannosidase II, swainsonine, resulted in change of the Fc oligosaccharide from complex type to hybrid type; culturing of Lec13 (in the presence of L-fucose) or Ms704 with swainsonine produced the Fu(+) hybrid type and the Fu(−) hybrid type, respectively (Figure 2D and E). Culture of Ms704 in the presence of a specific inhibitor of α-mannosidase I, kifunensine, yielded antihuman CD20 bearing high-mannose-type Fc oligosaccharides that included a relatively larger mannose moiety of 8 or 9 mannoses (M8,9) compared with the high-mannose type resulting from culture of the Lec1 cells, which included only 5 mannoses (M5) (Figure 2F and G).

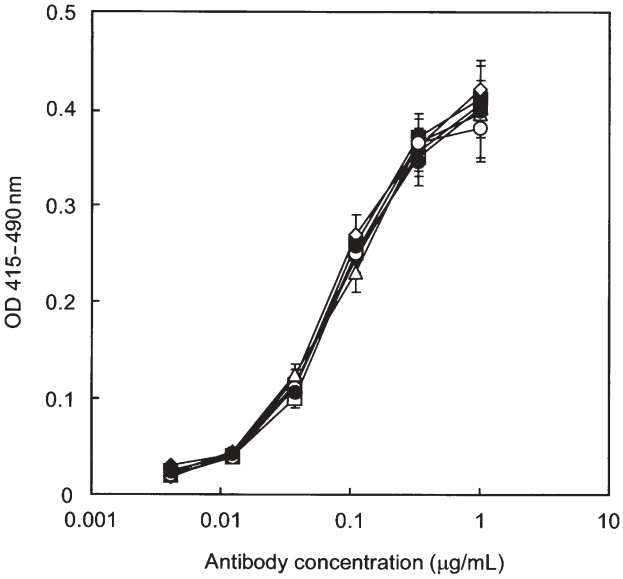

Fig. 1. Antigen-binding activity of antihuman CD20 IgG1s measured by ELISA. Human CD20$^+$ B lymphoma cell line Raji microsomes were coated and incubated with various concentrations of antibody. Goat antihuman IgG1 polyclonal antibodies were used to detect CD20 binding. The results shown are for the antibodies produced by Lec13 A4 with L-fucose (open squares), Ms704 1A7-15 (closed squares), Lec13 A4 with L-fucose and swainsonine (open diamonds), Ms704 1A7-15 with swainsonine (closed diamonds), Ms704 1A7-15 with kifunensine (open triangles), and Lec1 R7 (open circles). All produced antibodies showed the same antigen-binding affinity as rituximab (closed circles).

FcγRIIIa-binding activity

The human FcγRIIIa-binding activity of each purified antihuman CD20 was estimated by FcγRIIIa-binding ELISA and surface plasmon resonance measurement using the recombinant soluble human FcγRIIIa-His fusion protein (sFcγRIIIa). Both the FcγRIIIa allotype having high affinity (FcγRIIIa-158Val) and that having low affinity (FcγRIIIa-158Phe) to human IgG1 were expressed as sFcγRIIIa in the rat hybridoma cell line YB2/0. Compared with rituximab, which carries the Fu(+) complex-type Fc oligosaccharides, the only antihuman CD20 which showed weaker FcγRIIIa-binding activity was the Fu(+) hybrid type (Figure 3). The other types, including the Fu(−) complex type, the Fu(−) hybrid type, and the high-mannose types M5 and M8,9, exhibited significantly stronger binding activity for FcγRIIIa than the Fu(+) complex type (Figure 3). The binding kinetics analysis using a BIAcore^{TM} biosensor system T100 (BIACORE, Uppsala, Sweden) confirmed the difference observed in the FcγRIIIa-binding ELISA. The sensorgrams clearly showed that the Fu(+) hybrid type and the Fu(−) complex type have the weakest and the strongest binding affinities for FcγRIIIa, respectively (Figure 4). The Fu(−) hybrid type exhibited relatively higher FcγRIIIa-binding affinity than the Fu(+) complex type, and its sensorgram was similar to those of the high-mannose types M5 and M8,9 (Figure 4). The FcγRIIIa-binding affinity of each antihuman CD20 was calculated from steady-state analysis on the basis of the sensorgram, and the results are summarized in Table III. We used a receptor-capture sensor chip with an sFcγRIIIa-binding level of 700 resonance units (RU) to obtain the K_D values. The interaction of the Fu(+) hybrid type with the FcγRIIIa-158Phe allotype was so weak that it could not yield sufficient maximum signals (R_{max} values) for accurate data analysis, and thus the estimation of K_D was not possible for this interaction.

ADCC activity

The ADCC activity of each purified antihuman CD20 against the human CD20$^+$ B lymphoma cell lines, Raji and WIL2-S, was measured using human peripheral blood mononuclear cells (PBMC) as effector cells. Among the purified antihuman CD20s, the Fu(−) complex type and the Fu(+) hybrid type showed the strongest and the weakest ADCC,

Table I. Monosaccharide composition of *N*-linked oligosaccharides of antihuman CD20 IgG1s produced by CHO clones with/without glycosidase inhibitors

Relative composition of monosaccharides						
Clone	[a]Additive	[b]Fucose	GlcNAc	Mannose	Galactose	[c]Fucose (−)%
Lec13	LF	1.00	4.0	3.1	0.78	0
Lec13	LF/SW	1.00	3.0	4.9	0.68	0
Ms704		n.d.	4.0	2.6	0.59	100
Ms704	SW	n.d.	3.0	4.8	0.62	100
Ms704	KI	n.d.	2.0	8.8	n.d.	100
Lec1		n.d.	2.0	5.3	n.d.	100

[a]LF, L-fucose; LF/SW, L-fucose and swainsonine; KI, kifunensine.
[b]Molar ratios calculated versus GlcNAc composition.
[c]Total percentage of nonfucosylated oligosaccharides calculated by the formula (1 − a) × 100. n.d., not detected.

Table II. Summary of oligosaccharide analysis of antihuman CD20 IgG1s produced by CHO clones with/without glycosidase inhibitors

Relative composition of oligosaccharide (%)															
		Complex type						Hybrid type				High-mannose type			
Clone	[a]Additive	[b]a	b	c	d	e	f	g	h	i	j	k	l	m	Total (%)
Lec13	LF	54	42	4	—	—	—	—	—	—	—	—	—	—	100
Lec13	LF/SW	—	—	—	—	—	—	41	59	—	—	—	—	—	100
Ms704		—	—	—	63	34	3	—	—	—	—	—	—	—	100
Ms704	SW	—	—	—	—	—	—	—	—	44	56	—	—	—	100
Ms704	KI	—	—	—	—	—	—	—	—	—	—	19	81	—	100
Lec1		—	—	—	—	—	—	—	—	—	—	—	—	100	100

[a]LF, L-fucose; LF/SW, L-fucose and swainsonine; KI, kifunensine; —, not detected.
[b]Schematic oligosaccharide structures: galactose (open diamond); GlcNAc (closed circle); mannose (open square); fucose (open triangle).

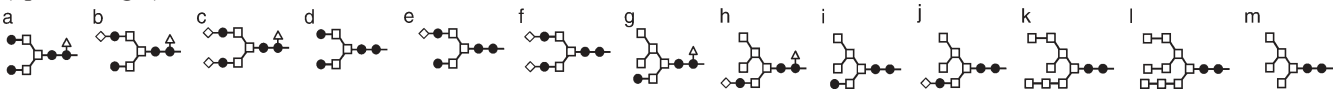

respectively (Figure 5A). There was no significant difference observed among the ADCC induced by the Fu(−) hybrid type and the high-mannose types M5 and M8,9 (Figure 5B). The ADCC induced by these three types was higher than that of the Fu(+) complex type. Thus, the effect of the Fc oligosaccharide glycoforms on ADCC well reflected their FcγRIIIa-binding affinity.

Next, the influence of Fu(+) antihuman CD20s of the hybrid type and the complex type on the ADCC of the Fu(−) complex type was investigated. A series of mixtures composed of the Fu(−) complex type and samples with different ratios was prepared to add serial 3-fold amounts of sample antihuman CD20 to an aliquot (3.7 ng/mL) of the Fu(−) complex type, and their ADCC values were measured. There was no significant change observed by the addition of the Fu(−) complex type, because the initial dose (3.7 ng/mL) was already above the saturation dose. On the other hand, the addition of the Fu(+) hybrid type as well as the Fu(+) complex type dramatically reduced the saturated ADCC efficacy of the Fu(−) complex type in a dose-dependent manner (Figure 6).

CDC activity

The CDC activity of each purified antihuman CD20 against the human $CD20^+$ B lymphoma cell line WIL2-S was measured using human serum as a complement source (Figure 7). There was no significant difference between the Fu(+) complex type and the Fu(−) complex type. The other types, the Fu(−) hybrid type, the Fu(+) hybrid type, and the high-mannose types M5 and M8,9, exhibited lower CDC than that of the complex type.

C1q-binding activity

To address the reason why change of the Fc oligosaccharide glycoforms from the complex type to the other types reduced CDC, we explored the binding ability of each purified antihuman CD20 to the complement component C1q on target cells (Figure 8). The amount of C1q bound on the target cells mediated by antihuman CD20 was increased in a dose-dependent manner when employing the complex type irrespective of core-fucosylation, whereas almost no bound C1q was detected when employing the other glycoforms in this experiment.

Pharmacokinetics in mice

Thirteen-week-old female ddY mice were injected intravenously with each purified antihuman CD20 lacking core-fucosylation, and the plasma clearances were monitored by a human IgG1-specific ELISA (Figure 9). The kinetics of elimination of the Fu(−) complex type was very similar to that of the Fu(+) complex type; approximately 50% to 60% of the administrated antihuman CD20 was cleared in the α-phase, and the remainder eliminated within the β-phase $t_{1/2}$ of approximately 14 days. In contrast, 60% to 70% of the Fu(−) hybrid type and the high-mannose type M5 was cleared in the α-phase, with the remainder showing an in vivo $t_{1/2}$ of 8.5 and 4.6 days, respectively.

FcRn-binding activity

The human FcRn-binding kinetics of each purified antihuman CD20 was estimated by surface plasmon resonance measurement using the BIAcore biosensor system. Because FcRn is a heterodimeric protein of a membrane-integral α-chain and a β2-microglobulin in which both chains make essential contacts with Fc, the recombinant soluble FcRn protein was expressed as the heterodimer and captured on a sensor chip. The sensorgrams of the different samples were highly similar, and no significant differences were detected. The FcRn affinity of each antihuman CD20 was calculated from bivalent model analysis on the basis of the sensorgram, and the results are summarized in Table IV. In all samples, the FcRn-binding affinity was decreased to below the detectable level when the experimental pH was changed from acidic (pH 6.0) to basic (pH 7.4) (data not shown).

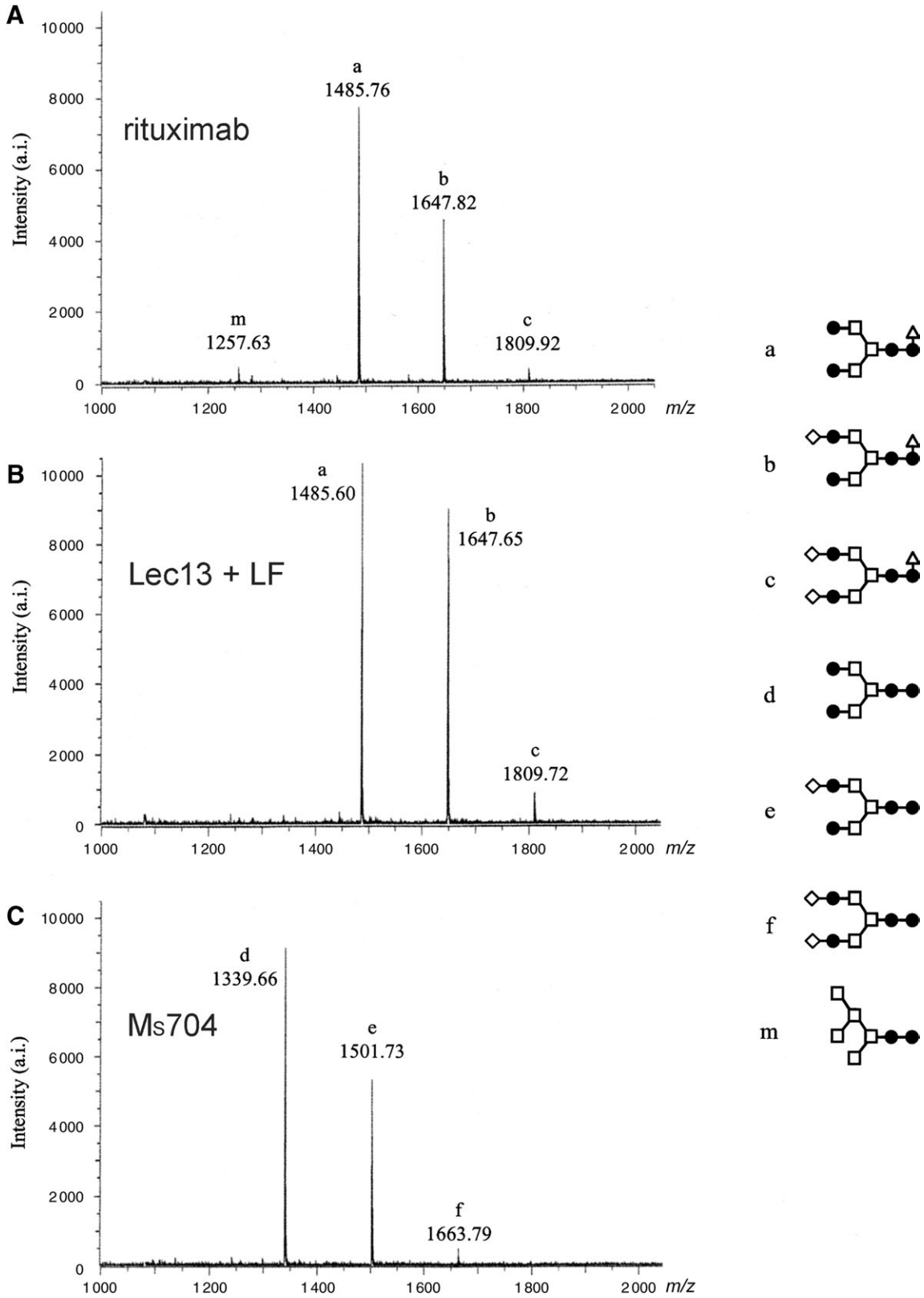

Fig. 2. MALDI-TOF MS spectra of neutral oligosaccharides from antihuman CD20 IgG1s. Antibody Fc oligosaccharides released by PNGase F digestion were analyzed using a MALDI-TOF MS spectrometer Reflex III. The m/z value corresponds to the sodium-associated oligosaccharide ion. Oligosaccharide structures of antihuman CD20s obtained from various CHO cell cultures are shown in each chart: (**A**) rituximab, (**B**) Lec13 A4 with L-fucose, (**C**) Ms704 1A7-15, (**D**) Lec13 A4 with L-fucose and swainsonine, (**E**) Ms704 1A7-15 with swainsonine, (**F**) Ms704 1A7-15 with kifunensine, and (**G**) Lec1 R7. The schematic oligosaccharide structure of each peak (from a to m) is illustrated on the right side of the charts: GlcNAc (closed circles), mannose (open squares), galactose (open diamonds), and fucose (open triangles).

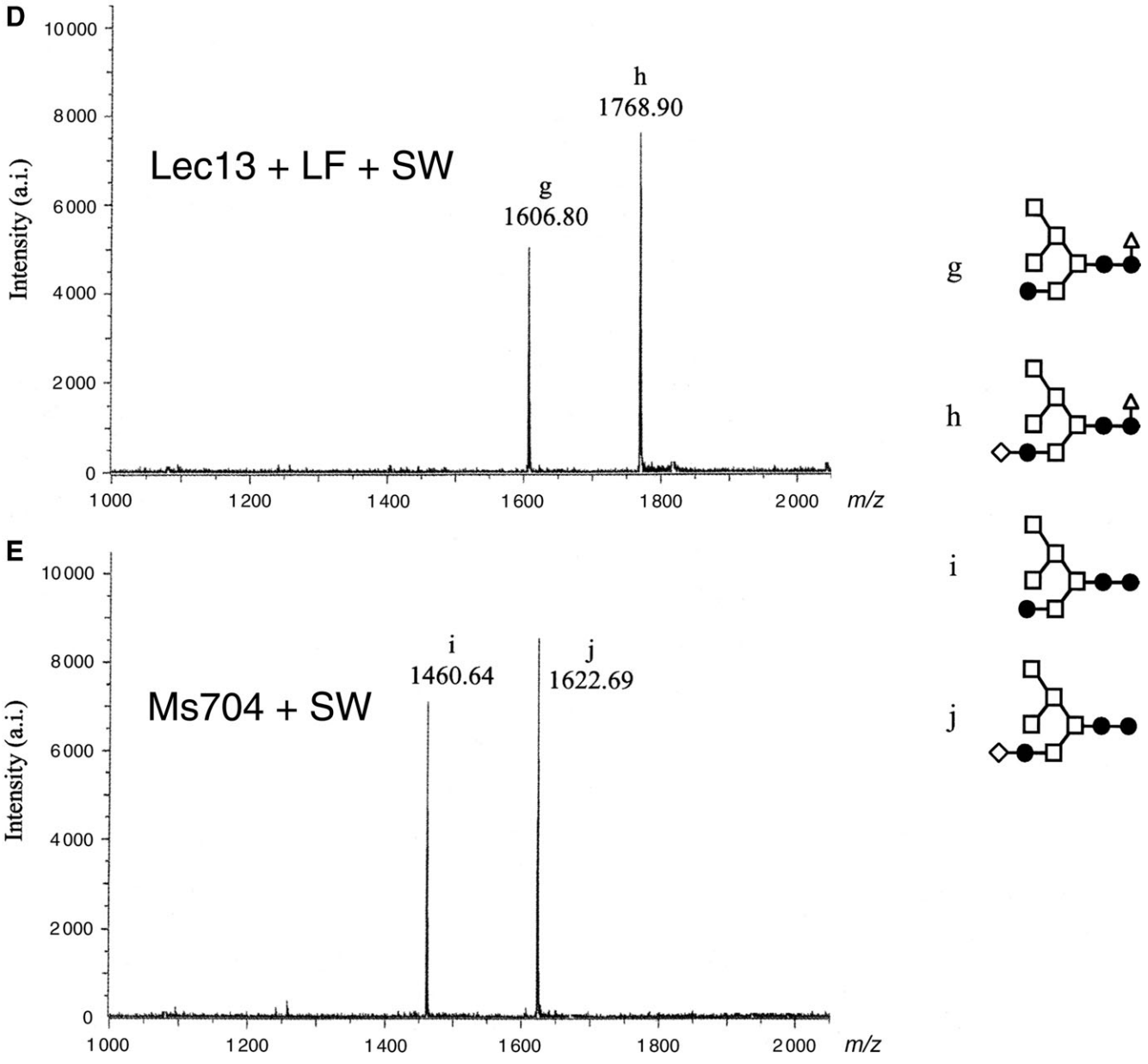

Fig. 2. Continued.

Discussion

Numerous studies have shown that the core-fucose residues of the C_H2-associated *N*-linked oligosaccharides play a critical role in the human IgG-mediated antibody effector function ADCC (Shields et al. 2002; Shinkawa et al. 2003; Niwa, Hatanaka et al. 2004; Niwa, Natsume et al. 2005; Niwa, Sakurada et al. 2005; Niwa, Shoji-Hosaka, et al. 2004; Okazaki et al. 2004; Jefferis 2005; Natsume et al. 2005; Iida et al. 2006). However, few studies have addressed the issue of how differences in the *N*-linked basic oligosaccharide structure affect the ADCC of the antibodies lacking the core-fucose residues. In this study, we have approached this basic problem by developing methods for generating nonfucosylated antibodies with three different *N*-linked Fc oligosaccharides, namely, a high-mannose, hybrid, and complex type, using the same producing clone.

To achieve our goal, we focused on mammalian cell lines with a defined defect in their glycosylation machinery and glycosidase inhibitors and extensively searched for combinations that could yield each of the desired oligosaccharide structures (Figure 2, Table II). Although a few cell lines have been reported to generate highly core-fucose-lacking (>90%) antibodies with the complex-type Fc oligosaccharides, the only cell line that is able to produce the completely nonfucosylated antibodies is a cell line lacking *FUT8* enzyme activity (Mori et al. 2004; Yamane-Ohnuki et al. 2004; Kanda et al. 2006). *FUT8* is known to be the only gene coding α-1,6-fucosyltransferase, which catalyzes the transfer of fucose from GDP-fucose to the GlcNAc residue of *N*-linked oligosaccharides (Uozumi et al. 1996;

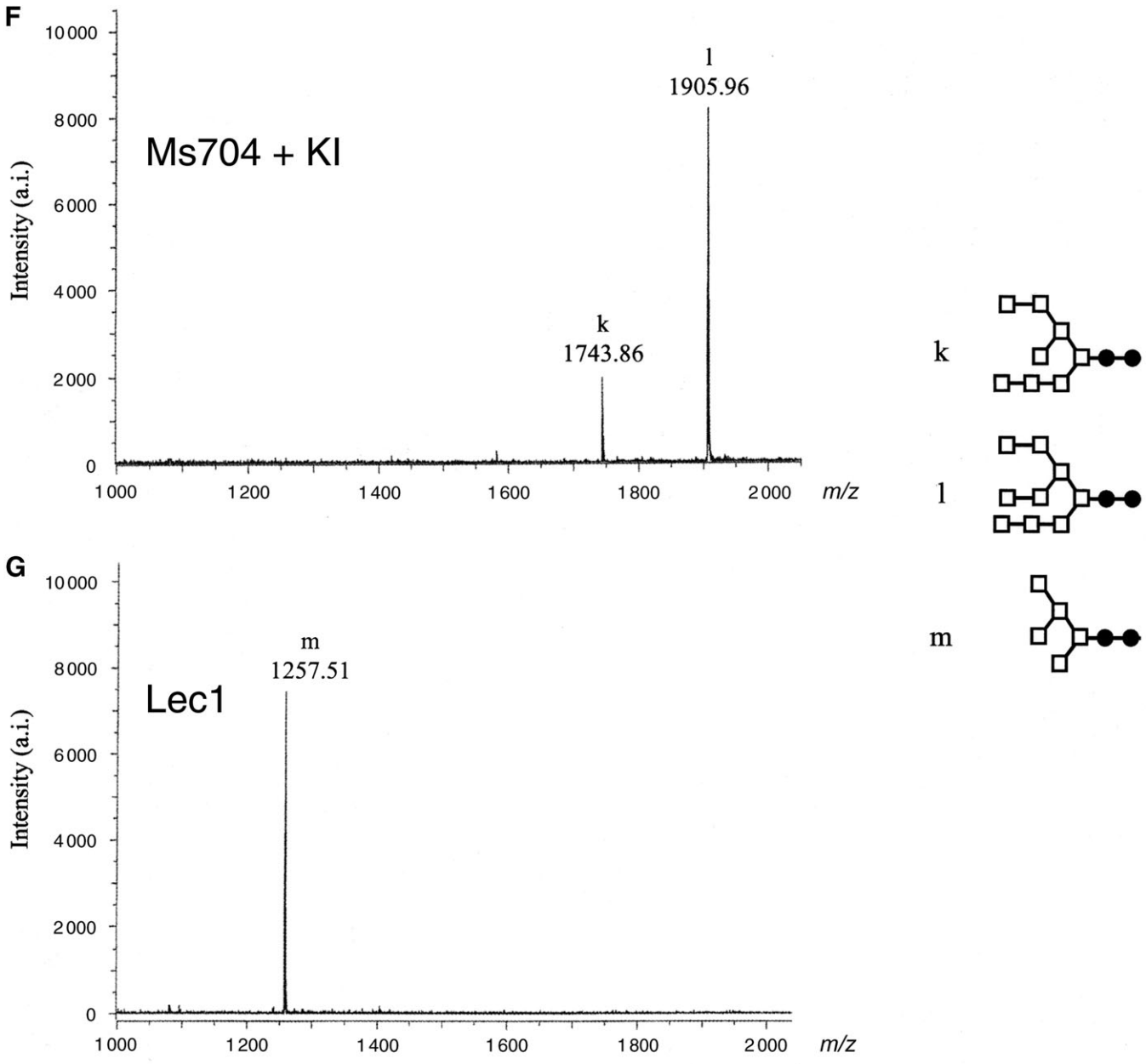

Fig. 2. Continued.

Yanagidani et al. 1997), and thus an *FUT8* knockout cell line would be theoretically unable to contribute the core-fucosylation. We therefore chose the *FUT8* knockout CHO cell line Ms704 as a host cell line to generate nonfucosylated antibodies with the three different *N*-linked Fc oligosaccharides. Antihuman CD20 IgG1, whose amino acid sequence is equivalent to that of rituximab, which has been licensed for the treatment of non-Hodgkin's lymphoma, was used as a model of recombinant therapeutic antibodies. In ordinary culture, *FUT8* knockout cells produced the nonfucosylated antibodies with the complex-type Fc oligosaccharides. The oligosaccharide change of the complex type to the high-mannose type was achieved by the cultivation with a glycosidase inhibitor specific to α-mannosidase I, kifunensine, resulting in production of nonfucosylated antibodies with the high-mannose type oligosaccharides comprising a relatively large mannose moiety of 8 or 9 mannoses. *FUT8* knockout cells were also able to produce nonfucosylated antibodies with the hybrid-type oligosaccharides when cultured in the presence of a glycosidase inhibitor specific to α-mannosidase II, swainsonine. Consequently, we succeeded in establishing a method for generating antibodies with each of the three different *N*-linked Fc oligosaccharides without contamination by any of the other types while maintaining the lack of core-fucosylation using the same producing clone.

The present method is distinct in several ways from the previously reported methods for changing the antibody oligosaccharides from the complex type to the other types. The inhibition of α-1,2-glucosidase I with castanospermine and

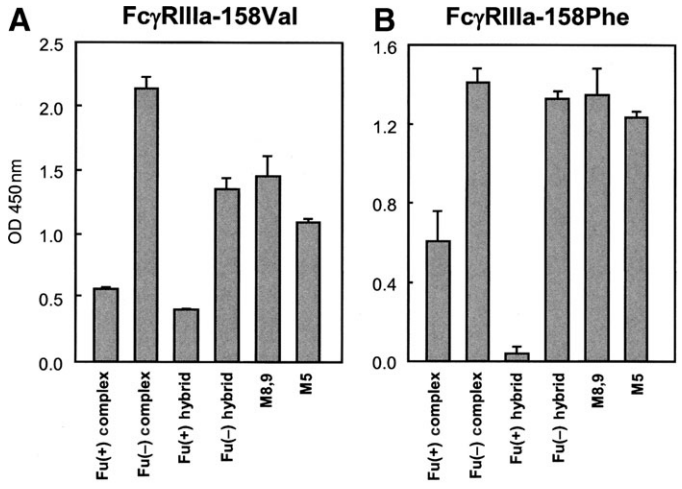

Fig. 3. FcγRIIIa-binding activity of anti-human CD20 IgG1s measured by ELISA. Goat antihuman IgG1 polyclonal antibodies were coated on 96-well immunoplates and incubated with equal amounts (0.5 μg/well) of sample antibodies and soluble human FcγRIIIa-His fusion protein [either (**A**) the FcγRIIIa-158Val allotype or (**B**) the FcγRIIIa-158Phe allotype]. The binding was detected by anti-Tetra·His antibody as the absorbance at 450 nm. Antihuman CD20s of the Fu(+) complex type, the Fu(−) complex type, the Fu(+) hybrid type, the Fu(−) hybrid type, and the high-mannose types M5 and M8,9 were employed as samples.

deoxynojirimycin yields the glucose-capped high-mannose-type oligosaccharides (Rothman et al. 1989; Awwad et al. 1990), and a *GnT-I*-deficient mutant CHO cell line Lec1 yields high-mannose-type oligosaccharides comprising a relatively small mannose moiety of 5 mannoses (Wright and Morrison 1994). In our experiments, detectable fucosylation of the high-mannose-type oligosaccharides from Lec1 was not observed. However, we may notice a possibility to modify the high-mannose-type oligosaccharides with fucose in Lec1, because Lec1 has been reported to generate the core-fucosylated high-mannose-type oligosaccharides (Lin et al. 1994; Crispin et al. 2006). Two different approaches have been reported for the generation of nonfucosylated antibodies with the hybrid-type Fc oligosaccharides. Treatment of antibody-producing cells with monensine causes the Fc oligosaccharide structure change from the core-fucosylated complex type to the nonfucosylated hybrid type (Rothman et al. 1989). The mechanism mediated by monensine is still unclear, though it appears that monensine functions as an intracellular protein traffic inhibitor. Overexpression of *GnT-III* in antibody-producing cells also causes the addition of bisected GlcNAc to the Fc oligosaccharides with increased population of the nonfucosylated hybrid type, which is thought to disturb *N*-linked oligosaccharide processing in Golgi apparatus, and eventually increases the amount of the nonfucosylated hybrid type (Schuster et al. 2005; Ferrara, Brunker et al. 2006; Ferrara, Stuart et al. 20062). Both approaches, however, failed to change to the nonfucosylated hybrid type without contamination of other glycoforms; a certain amount of the complex type and the hybrid type with the core-fucose residues, which influence the biological activity of antibodies lacking the core-fucose residues (Figure 6), also remained in their products.

Biological activity analysis of our prepared antihuman CD20 IgG1s with three different *N*-linked Fc oligosaccharides confirmed previous reports (Rothman et al. 1989; Awwad et al. 1990; Nose and Heyman 1990; Wright and Morrison 1994, 1998; Yamane-Ohnuki et al. 2004; Schuster et al. 2005) and revealed several new findings. First, the effect of the Fc oligosaccharide structures on the binding affinity of human IgG1 to human FcγRIIIa were quantified; the nonfucosylated complex type had the strongest FcγRIIIa-binding activity and induced the strongest ADCC mediated by human PBMC. On the other hand, the core-fucosylated hybrid type had both the weakest FcγRIIIa-binding activity and the weakest ADCC, which was firstly disclosed this time. The other types, the nonfucosylated hybrid type and the high-mannose types M5 and M8,9, had moderate and relatively higher FcγRIIIa-binding activity and ADCC than the fucosylated complex type, and there were no significant differences among them. Secondly, human IgG1 with the complex type induced the strongest human C1q-binding activity and CDC irrespective of core-fucosylation. In the hybrid type, the fucosylated form also showed a level of activity equivalent to the nonfucosylated form. The CDC mediated by the hybrid type, which was relatively lower than that of the complex type, was comparable with the activity by the high-mannose type. It was interesting to find that C1q binding and CDC were not affected by core-fucosylation of the Fc oligosaccharides. Thus, the structure of the nonreducing end of *N*-linked Fc oligosaccharides seems to be critical for C1q binding and CDC, whereas the reducing-end structure, in which the fucose is attached to the innermost GlcNAc of *N*-linked Fc oligosaccharides, is important in reducing FcγRIIIa binding and ADCC. The bulky structure commonly observed in the nonreducing end between the hybrid type and the high-mannose type may influence the structure of the Fc region interacting with C1q, a huge hexamer containing six globular heads attached to six collagen-like tails. Our quantitative data of how the refined differences in the *N*-linked Fc oligosaccharide structure affect the effector functions of human IgG1 will facilitate conformational structure study of complexes of antibody and its effector ligands.

Generally, oligosaccharides are thought to play a role in in vivo glycoprotein targeting and clearance. Glycoproteins with exposed sugar residues such as galactose and mannose are known to be trapped by the specific receptors on hepatocytes and macrophages (Thornburg et al. 1980; Malaise et al. 1990; Wright et al. 2000). In the case of antibody, atypical Fc oligosaccharides such as the high-mannose type appear to be at least partially exposed, although the biantennary complex-type Fc oligosaccharides of IgG are normally buried between the C_H2 domains of the two heavy chains (Huber et al. 1976; Tao et al. 1993; Harris et al. 1998; Radaev et al. 2001). Actually, rapid clearance of the high-mannose type from Lec1 has been demonstrated and shown to be inhibited by the co-injection of yeast mannan (Wright and Morrison 1994). We confirmed that the high-mannose type had the shortest in vivo half-life in mice, followed by the hybrid type, which seems to well reflect the theory of clearance depending on the number of exposed galactose and mannose residues. In the complex type, there was no significant difference of the clearance between the core-fucosylated and nonfucosylated forms in mice. Human IgG1 antibodies are characterized by long-term stability in

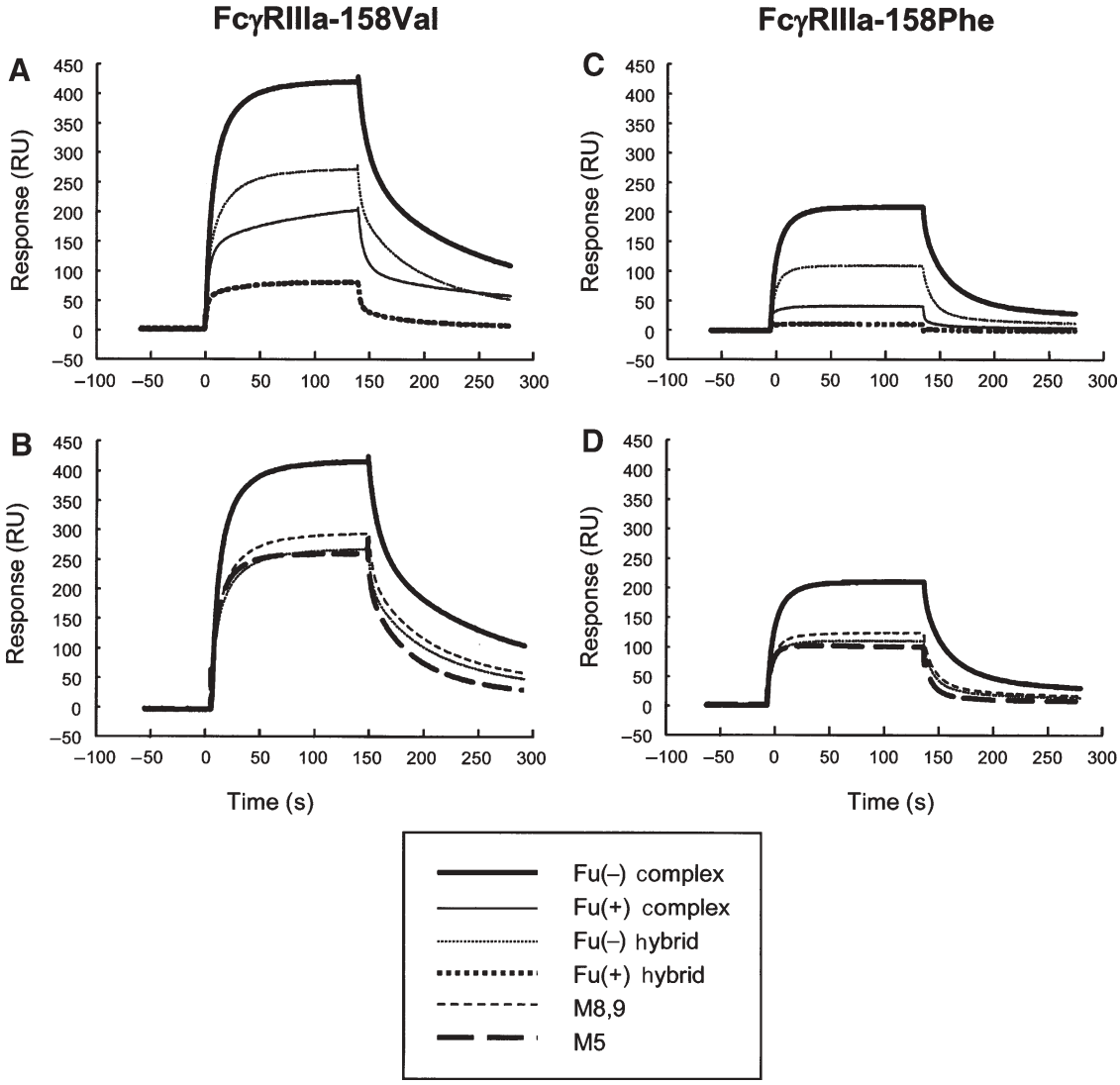

Fig. 4. Surface plasmon resonance analysis of FcγRIIIa binding of antihuman CD20 IgG1s. Antihuman CD20s of the Fu(−) complex type (bold continuous line), the Fu(−) hybrid type (dotted line), the Fu(+) complex type (continuous line), the Fu(+) hybrid type (bold dotted line), the high-mannose type M8,9 (dashed line), and the high-mannose type M5 (bold dashed line) were injected over either the sFcγRIIIa-158Val [(**A**) and (**B**)] or the sFcγRIIIa-158Phe [(**C**) and (**D**)] capture sensor chip. The concentrations of injected antihuman CD20s were 133.3 nM. In a control experiment, buffer solution without antihuman CD20s was injected over the receptor-capture sensor chip. The sensorgram obtained from the control experiment was subtracted form the sensorgrams obtained by the antihuman CD20 injection to yield the curves presented in the figure.

Table III. Human FcγRIIIa-binding affinity of antihuman CD20 IgG1s produced by CHO clones from steady-state analysis using a BIAcore biosensor system

Antibody	K_D for allotype FcγRIIIa-158Val ($\times 10^{-8}$ M)	K_D for allotype FcγRIIIa-158Phe ($\times 10^{-8}$ M)
Fu(+) complex	12.95	53.30
Fu(−) complex	4.94	9.40
Fu(+) hybrid	34.31	n.d.
Fu(−) hybrid	8.43	18.32
M5	8.57	22.10
M8,9	6.70	14.28

n.d., not detected.

human blood (approximately 21 days) via a unique FcRn mechanism (Junghans and Anderson 1996; Ober et al. 2004). An equivalent FcRn-binding affinity was observed among the human IgG1s with three different *N*-linked Fc oligosaccharides irrespective of the structural differences. Therefore, the trends in clearance observed in mice in the present study are considered to reflect the clearance of the IgGs in humans in vivo to some extent.

In conclusion, we succeeded in developing a method for generating antibodies that completely lacked core-fucose residues and that had one of three different *N*-linked Fc oligosaccharides attached, i.e. a high-mannose type, hybrid type, or complex type, and directly compared their biological activities. The *FUT8* knockout CHO cell line was suitable for this purpose, because it yields distinguishable production of each type. Contamination by any of the other types of antibody

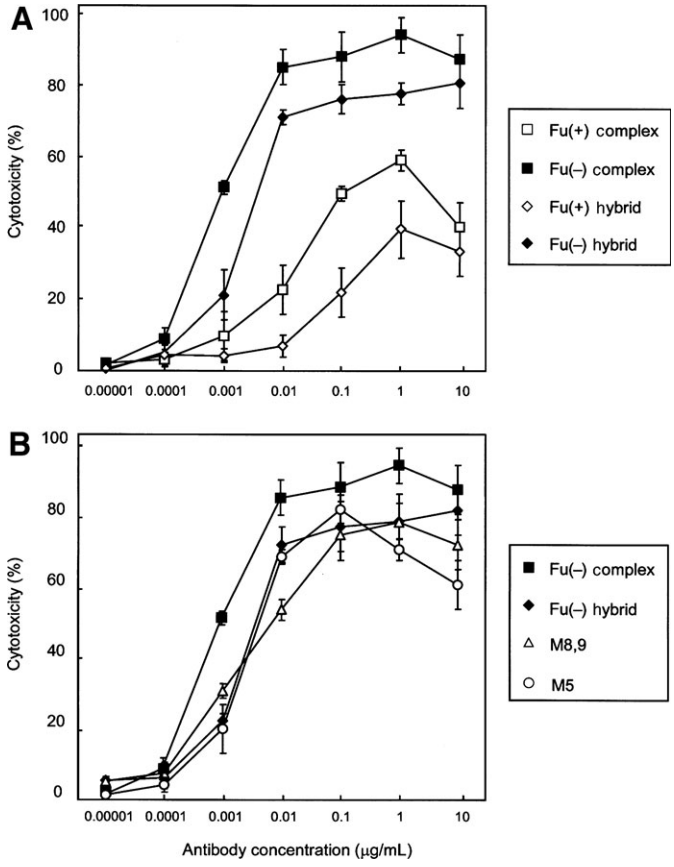

Fig. 5. ADCC activity of antihuman CD20 IgG1s. Cytotoxicity against human $CD20^+$ B lymphoma cell line Raji cells was induced by the corresponding antihuman CD20s. All experiments were done by a ^{51}Cr release assay using human PBMC as effector cells at an E/T ratio of 20/1. The cytotoxicities (%) are presented as the mean values ± SD of triplicate experiments. Antihuman CD20s of the Fu(+) complex type (open squares), the Fu(−) complex type (closed squares), the Fu(+) hybrid type (open diamonds), the Fu(−) hybrid type (closed diamonds), and the high-mannose types M5 (open circles) and M8,9 (open triangles) were employed as samples. Comparable data were obtained when WIL2-S cells were employed as target cells (data not shown).

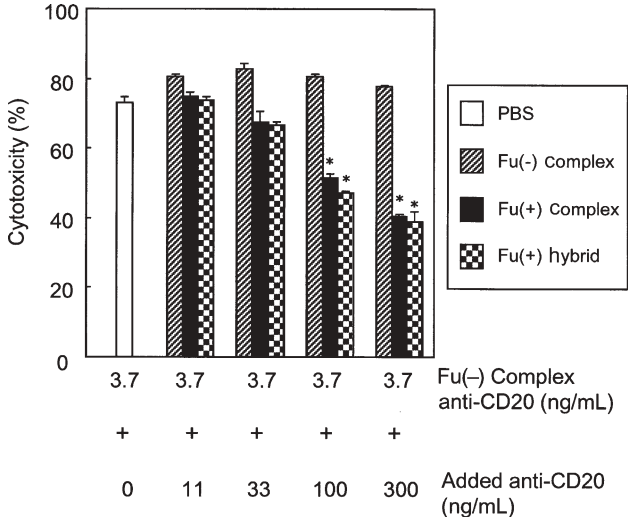

Fig. 6. Influence of antihuman CD20 with the Fu(+) complex type or hybrid type Fc oligosaccharides on ADCC of the Fu(−) complex-type anti-human CD20. The Fu(−) complex-type anti-human CD20 was added to the culture at 3.7 ng/mL. The corresponding antihuman CD20 [the Fu(−) complex type (▨), the Fu(+) complex type (■), the Fu(+) hybrid type (▩), or PBS alone (□)] was further added to the reaction at the indicated concentrations. The values plotted as the abscissa show the concentrations of the Fu(−) complex type, the Fu(+) complex type, and the Fu(+) hybrid type added to the reaction. All experiments were done by a ^{51}Cr release assay using human PBMC as effector cells and cells of the human $CD20^+$ B lymphoma cell line Raji as target cells at an E/T ratio of 20/1. The cytotoxicities (%) are indicated as the mean values ± SD of triplicate experiments. $^*P < 0.05$ compared with the ADCC value in the absence of added antihuman CD20s, as determined by the Student paired t test.

could lead to an inaccurate estimation of biological activity, because these different types of antibodies compete with each other. For instance, the fucosylated forms of the hybrid type as well as those of the complex type have been shown to inhibit the high ADCC induced by the nonfucosylated complex type, probably due to competition for the antigen on target cells (Iida et al. 2006). The present study revealed basic information regarding the effect of *N*-linked oligosaccharide structures on the antibody effector functions and pharmacokinetics of human IgG1 lacking core-fucose residues, which will be useful for improving the physiological activity of the human IgG1s widely used as therapeutic reagents.

Materials and methods

Materials

Swainsonine (a specific inhibitor of α-mannosidase II) and kifunensine (a specific inhibitor of α-mannosidase I) were

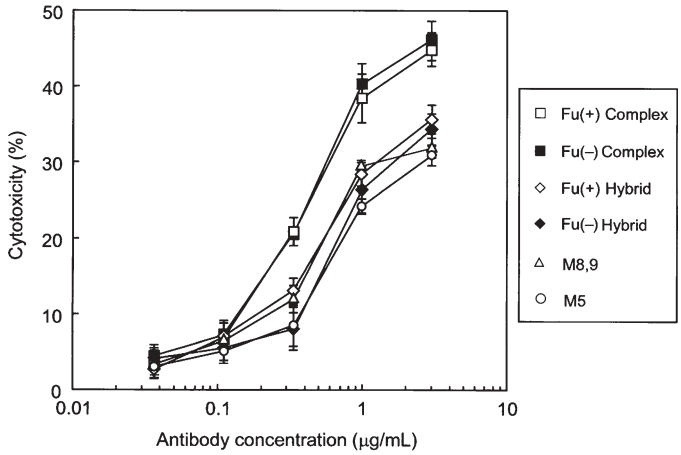

Fig. 7. CDC activity of antihuman CD20 IgG1s. Cytotoxicity against human $CD20^+$ B lymphoma cell line WIL2-S cells was induced by the human serum complement in the presence of the corresponding antihuman CD20s. Cytotoxicities (%) are indicated as the mean values ± SD of triplicate experiments. Antihuman CD20s of the Fu(+) complex type (open squares), the Fu(−) complex type (closed squares), the Fu(+) hybrid type (open diamonds), the Fu(−) hybrid type (closed diamonds), and the high-mannose types M5 (open circles) and M8,9 (open triangles) were employed as samples.

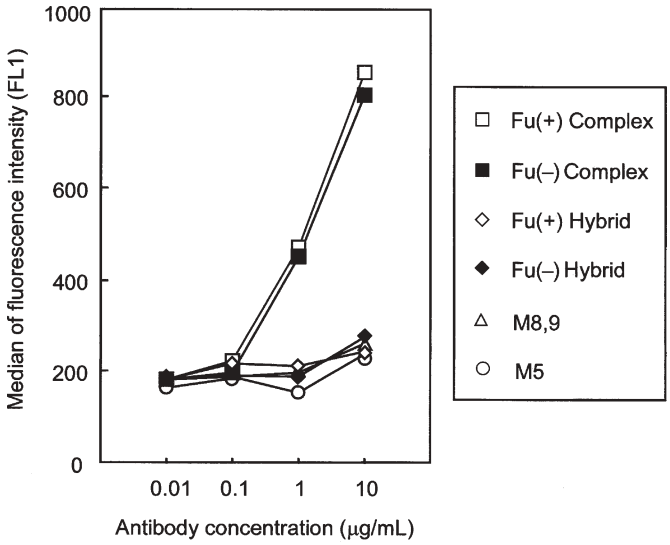

Fig. 8. C1q-binding activity of antihuman CD20 IgG1s. The C1q binding on human $CD20^+$ B lymphoma cell line WIL2-S cells induced by the corresponding antihuman CD20s was measured by flow cytometry. The binding ability was represented as the median fluorescence intensity. Antihuman CD20s of the Fu(+) complex type (open squares), the Fu(−) complex type (closed squares), the Fu(+) hybrid type (open diamonds), the Fu(−) hybrid type (closed diamonds), and the high-mannose types M5 (open circles) and M8,9 (open triangles) were employed as samples.

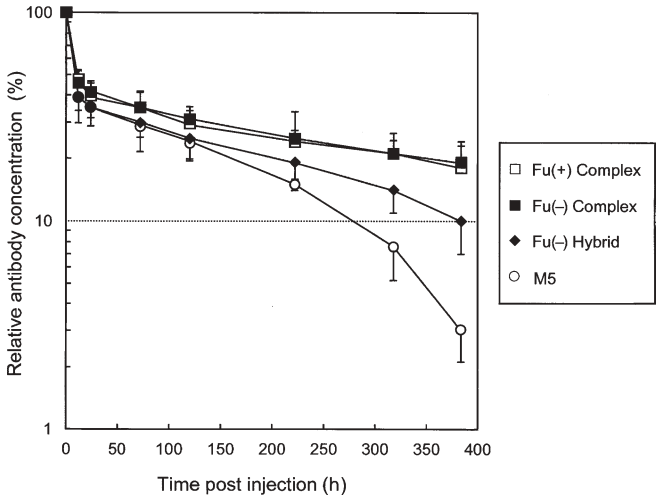

Fig. 9. Plasma clearance of antihuman CD20 IgG1s in mice. Female ddY mice were injected intravenously with antihuman CD20s. The antibody concentrations in plasma were monitored using a human IgG-specific ELISA. The data shown are the averages for three treated mice as a percentage of the dose remaining over time (the serum concentration 5 min after injection is regarded as 100%). The serum half-life was calculated from the elimination β-phase. Antihuman CD20s of the Fu(+) complex type (open squares), the Fu(−) complex type (closed squares), the Fu(−) hybrid type (closed diamonds), and the high-mannose type M5 (open circles) were employed as samples.

purchased from Sigma-Aldrich (St Louis, MO). L-fucose was obtained from Wako Pure Chemical Industries (Osaka, Japan). Antihuman CD20 mouse/human chimeric IgG1 rituximab (Rituxan®) was purchased from Genentech, Inc. (South San Francisco, CA)/IDEC Pharmaceutical (San Diego, CA).

Table IV. Human FcRn-binding affinity of antihuman CD20 IgG1s produced by CHO clones from bivalent model analysis using a BIAcore biosensor system

Antibody	Association constant k_a ($\times 10^5$ $M^{-1}s^{-1}$)	Dissociation constant k_d (s^{-1})	Affinity K_D ($\times 10^{-7}$ M)
Fu(+) complex	10.70	0.70	6.5
Fu(−) complex	4.71	0.19	4.0
Fu(+) hybrid	4.14	0.18	4.3
Fu(−) hybrid	3.97	0.15	3.7
M5	4.06	0.16	3.9
M8,9	4.18	0.15	3.5

Cell lines

The dihydrofolate reductase-deficient CHO cell line, CHO/DG44 (Urlaub and Chasin 1980), was obtained from Dr Lawrence Chasin, Columbia University, NY. The variant CHO cell line deficient in endogenous *GMD*, Pro-Lec13.6A (Lec13) (Ripka et al. 1986), was provided by Dr Pamela Stanley, Albert Einstein College of Medicine, Yeshiva University, NY. The variant CHO cell line deficient in endogenous GnT-*I*, Pro-5WgaRI3C (Lec1) (Stanley and Chaney 1985), was purchased from the American Type Culture Collection (ATCC, Manassas, VA). The *FUT8* knockout CHO cell line, Ms704 (Yamane-Ohnuki et al. 2004), was established in our laboratory. All CHO cell lines were maintained in Iscove's modified Dulbecco's medium (Invitrogen, Carlsbad, CA) containing 10% (v/v) dialyzed fetal bovine serum (Invitrogen), 0.1 mM hypoxanthine, and 16 μM thymidine (Invitrogen). The human $CD20^+$ B lymphoma cell lines, Raji and WIL2-S, were purchased from ATCC and cultured in RPMI1640 media (Invitrogen) containing 10% (v/v) fetal bovine serum (Invitrogen).

Antibody-producing cells

Two antibody-producing clones, Lec13 A4 and Ms704 1A7-15, transformed by the antihuman CD20 mouse/human chimeric IgG1 (equivalent to rituximab) expression vector pKANTEX2B8P (Shinkawa et al. 2003), were established as described previously (Kanda et al. 2006). The same expression vector was transfected into Lec1, and a G418-resistant transfectant was selected as Lec1 R7 on the basis of antibody production. The antibody concentration in the culture supernatant was measured by an ELISA specific for human IgG1 as described previously (Nakamura et al. 2000).

Preparation of glycoengineered antibodies

Three antihuman CD20 IgG1-producing clones, Lec13 A4, Ms704 1A7-15, and Lec1 R7, were expanded in tissue culture flasks (Greiner, Kremsmünster, Austria) and grown to confluence. The confluent clones were rinsed twice with the Dulbecco's phosphate-buffered saline (PBS) (Invitrogen) and cultured in serum-free medium EX-CELL™ 301 (JRH Biosciences, Lenexa, KS) at 37 °C in an atmosphere of 5% CO_2 (v/v) for 1 week in the presence or absence of either L-fucose (1 mM), swainsonine (60 μM), or kifunensine

(20 μM). IgG1s were purified from the culture media using MabSelect^{TM} (Amersham Biosciences, Piscataway, NJ) and stored in 10 mM citrate buffer (pH 6.0) with 0.15 M NaCl. The purity and integrity of each purified IgG1 was confirmed by SDS–PAGE. The protein concentration of the purified IgG1s was measured by absorbance at 280 nm.

Analysis of antibody-derived N-linked Fc oligosaccharides

The monosaccharide composition of each purified IgG1 was characterized by modified high-performance anion exchange chromatography; monosaccharides were released from an aliquot of IgG1 by heating with 4 M trifluoroacetic acid at 100 °C for 2 h and dried under a vacuum. The monosaccharides reconstituted in sterile distilled water were analyzed using a waveform and DX500 system (DIONEX, Sunnyvale, CA). A CarboPac PA-1 column (DIONEX) was used to resolve monosaccharides in 18 mM sodium hydroxide solution with a flow rate of 0.8 mL/min at 35 °C as described previously (Shinkawa et al. 2003).

The oligosaccharide profile of each purified IgG1 was characterized by modified matrix-assisted laser desorption/ionization time-of-flight mass spectrometry (MALDI-TOF MS) with a positive ion mode as described previously (Papac et al. 1998); *N*-linked oligosaccharides were released from 30 μg of IgG1 by incubation with 1 unit of recombinant peptide-*N*-glycosidase F (PNGaseF; Sigma-Aldrich) for 18 h at 37°C in 10 mM Tris-acetate (pH 8.3). The released oligosaccharides were recovered after precipitation of the protein with 75% ethanol. Following drying of the recovered supernatant, the oligosaccharides were dissolved in 13 mM acetic acid and incubated at room temperature for 2 h. The acid-treated samples were desalted with cation-exchange resin (AG50W-X8, hydrogen form; BioRad, Hercules, CA) and dried in a vacuum. The dried samples were dissolved in deionized water and mixed with the matrix super-DHB solution (Bruker Daltonics) to be characterized by a MALDI-TOF MS spectrometer Reflex III (Bruker Daltonik GmbH, Bremen, Fahrenheitstr, Germany) equipped with delayed extraction. All samples were irradiated with ultraviolet light (337 nm) from an N_2 laser; positive ions were accelerated to 20 kV and analyzed in a reflectron mode. The oligosaccharide standards (TAKARA BIO Inc., Shiga, Japan) were employed.

Antigen-binding assay

The antigen-binding activity of antihuman CD20 IgG1 was measured by a CD20-binding ELISA as described previously (Yamane-Ohnuki et al. 2004). Immunofluorescence staining of the human CD20$^+$ B lymphoma cell line Raji was also performed using a FACSCalibur flow cytometer (BD Biosciences, San Jose, CA). Cells were adjusted to 4×10^6 cells/mL and incubated with 2 μg/mL antibody for 30 min in an ice-cold stain buffer [PBS containing 1% bovine serum albumin (BSA)]. The cells were then washed and incubated with phycoerythrin-conjugated mouse antihuman IgG (BD Biosciences Pharmingen, San Diego, CA) for 30 min to detect antibody binding. Antihuman CD20 mouse/human chimeric IgG1 rituximab was employed as a control.

FcγRIIIa-binding assay

The binding affinity of each purified IgG1 for human FcγRIIIa was measured by a FcγRIIIa-binding ELISA as described previously (Yamane-Ohnuki et al. 2004). The binding kinetics of IgG1 to FcγRIIIa was measured using a BIAcore T100 instrument and CM5 sensor chips (BIACORE, Uppsala, Sweden) as follows. Anti-Tetra·His antibody (Qiagen, Hilden, Germany) was immobilized onto the BIAcore sensor chip using an amine-coupling kit (BIACORE) following the manufacturer's instructions. Another sensor chip was treated with carbodimide/ethanolamine instead of the anti-Tetra·His antibody to produce a reference surface. Soluble recombinant FcγRIIIa carrying a hexa-His tag, produced by the rat hybridoma cell line YB2/0 as described previously (Niwa, Hatanaka et al. 2004; Yamane-Ohnuki et al. 2004), was captured by the immobilized anti-Tetra·His antibody by injecting the soluble FcγRIIIa at a flow rate of 5 μL/min. The purified antihuman CD20 IgG1s were diluted in HBS-EP buffer (0.01 M HEPES, 0.15 M NaCl, 3 mM EDTA, 0.005% Surfactant P20, pH 7.4) at six different concentrations (from 4.17 to 133.3 nM) and each diluted IgG1 was injected over the receptor-captured sensor surface at a flow rate of 5 μL/min. The experiments were performed at 25 °C with HBS-EP as the running buffer. Buffer solution without sample IgG1 was injected over the receptor-captured sensor surface as a blank control. Soluble FcγRIIIa and IgG1 bound to the sensor surface were removed by injecting 7.5 mM HCl at a flow rate of 10 μL/min for 30 s. The data obtained by the injection of IgG1 were corrected for the blank control prior to data analysis. An affinity (K_D) for FcγRIIIa was calculated by steady-state analysis using BIAcore T100 kinetic evaluation software (BIACORE).

C1q-binding assay

The ability of each purified antihuman CD20 IgG1 to bind to the C1q component of the complement was studied by a flow cytometric assay using purified human complement C1q. Human CD20$^+$ B lymphoma WIL2-S cells were adjusted to 2×10^6 cells/mL and incubated with serial dilutions of antihuman CD20 IgG1 for 30 min in a stain buffer [PBS containing 1% (w/v) BSA]. After washing with the stain buffer, purified human complement C1q (Biogenesis Ltd, Poole, UK) was added at a final concentration of 20 μg/mL and bound to the cell-bound antihuman CD20 IgG1s at 37 °C for 30 min. Cells were then washed and incubated with fluorescein isothiocyanate-conjugated polyclonal antibodies against human C1q (Acris Antibodies GmbH, Hiddenhausen, Germany) for 30 min. Stained cells were analyzed by flow cytometry using FACSCalibur.

FcRn-binding assay

Human neonatal Fc receptor (FcRn) α-chain cDNA was cloned from human placenta cDNA (CLONTECH, Mountain View, CA) by polymerase chain reaction and modified by replacing the transmembrane and intracellular domains with a hexa-His tag and then subcloned into the mammalian cell expression vector pKANTEX93 (*Eco*RI/*Dra*III) (Nakamura et al. 2000). Human β2-microglobulin cDNA was also subcloned into the same vector (*Not*I/*Bam*HI). The recombinant soluble FcRn-β2 microglobulin complex was expressed in

CHO/DG44 cells and purified from the culture supernatant by Ni-NTA chromatography (Qiagen). The kinetics of the human IgG1–FcRn interaction was measured using a BIAcore T100 instrument and CM5 sensor chips. Antihuman β2-microglobulin monoclonal antibody (Abcam, Cambridge, UK) was immobilized onto the chip using an amine-coupling kit (BIACORE). Soluble FcRn-β2 microglobulin complex was captured by the immobilized anti-β2-microglobulin antibody by injecting the complex at a flow rate of 5 μL/min. Buffer solution without the complex was injected over the antibody-captured sensor surface as a blank control. Each purified antihuman CD20 IgG1 was diluted in HBS-EP+ buffer (0.01 M HEPES, 0.15 M NaCl, 3 mM EDTA, 0.05% Surfactant P20) whose pH was adjusted to 6.0 at five different concentrations (from 4.17 to 66.7 nM), and each diluted IgG1 was injected over the complex-captured sensor surface or blank at a flow rate of 5 μL/min. Soluble FcRn and IgG1 bound to the sensor surface were removed by injecting 7.5 mM HCl at a flow rate of 60 μL/min for 1 min. The experiments were performed at 25 °C with HBS-EP+ as a running buffer. The data obtained by blank subtraction were used for the data analysis. An apparent association rate constant (k_a), a dissociation rate constant (k_d), and the binding affinity (K_D) were calculated by the bivalent fitting model using BIAcore T100 evaluation software.

ADCC assay

ADCC activity was determined by the ^{51}Cr release assay as reported previously (Ohta et al. 1993). Briefly, the human $CD20^+$ B lymphoma cell lines Raji or WIL2-S as the target cells were labeled with 3.7 MBq of $Na_2^{51}CrO_4$ at 37 °C for 1 h. Human PBMC purified from healthy donors, using Lymphoprep (Nycomed Pharma AS, Roskilde, Norway), were used as effector cells and mixed with the ^{51}Cr-labeled target cells at an E/T ratio of 20/1 in the presence of corresponding antihuman CD20 IgG1s. After incubation at 37 °C for 4 h, the radioactivity in the supernatants was measured using a γ counter (Beckman Coulter, Fullerton, CA). The percentage of specific cytolysis was calculated from the counts of samples according to the formula: $\%\text{cytotoxicity} = 100 \times (E - S)/(M - S)$, where E represents the experimental release (cpm in the supernatant from target cells incubated with antibody and effector cells), S is the spontaneous release (cpm in the supernatant from target cells incubated with medium alone), and M is the maximum release (cpm released from target cells lyzed with 1 mol/L hydrochloric acid). The ability of each sample IgG1 to inhibit the ADCC of anti-human CD20 IgG1 of the nonfucosylated complex type was measured as reported previously (Iida et al. 2006).

CDC assay

CDC activity was determined by the WST-1 assay as reported previously (Yamane-Ohnuki et al. 2004). Briefly, target human $CD20^+$ B lymphoma WIL2-S cells (5×10^4), 2-fold diluted human serum complement (Sigma-Aldrich), and serial dilutions of antihuman CD20 IgG1 were incubated in 96-well flat-bottomed plates (Greiner) for 1 h at 37 °C. WST-1 reagent (Roche Diagnostics, Basel, Switzerland) was added to the wells (15 − L/well) and incubated for 6 h at 37 °C. Absorbance in the wells was measured at 450 nm using a Benchmark microplate reader (BioRad, Hercules, CA) and expressed in relative absorbance units (RAU) as an index of the viable cell number. The percent CDC was calculated according to the formula: $\%\text{CDC activity} = 100 \times (\text{RAU background} - \text{RAU test})/\text{RAU background}$.

Pharmacokinetic analysis in mice

For each purified antihuman CD20 IgG1, three 13-week-old female ddY mice (Charles River Laboratories, Kanagawa, Japan) were injected into the tail vein with 20 μg of the IgG1. Peripheral blood samples (40 L) were taken from the tail vein at 0.083 (5 min), 0.5, 1, 6, 24, 60, 120, 216, 312, and 384 h, and the antibody concentration in the plasma was measured by an ELISA specific for human IgG1 as described previously (Nakamura et al. 2000). The serum half-life of the administrated IgG1 was calculated from the slope of the elimination β-phase.

Acknowledgments

The authors thank Dr Lawrence Chasin and Dr Gail Urlaub Chasin (Columbia University) for their generous gift of the CHO/DG44 cell line, and Dr Pamela Stanley (Albert Einstein College of Medicine, Yeshiva University) for her kind gift of the Lec13 cell line.

Conflict of interest statement

None declared.

Abbreviations

ADCC, antibody-dependent cellular cytotoxicity; BSA, bovine serum albumin; CDC, complement-dependent cytotoxicity; CHO, Chinese hamster ovary; ELISA, ezyme-linked immunosorbent assay; GDP, guanosine diphosphate; *GMD*, GDP-mannose 4,6-dehydratase; GnT-I, N-acetylglucosaminlytransferase I; *GnT*-III, β-1,4-N-acetylglucosaminyltransferase III; IgG1, immunoglobulin G1; MALDI-TOF MS, matrix-assisted laser desorption/ionization time-of-flight mass spectrometry; PBMC, peripheral blood mononuclear cells; PBS, phosphate-buffered saline; NK, natural killer; RAU, relative absorbance units; SDS–PAGE, sodium dodecyl sulfate polyacrylamide electrophoresis

References

Awwad M, Strome PG, Gilman SC, Axelrod HR. 1994. Modification of monoclonal antibody carbohydrates by oxidation, conjugation, or deoxymannojirimycin does not interfere with antibody effector functions. Cancer Immunol Immunother. 38:23–30.

Crispin M, Harvey DJ, Chang VT, Yu C, Aricescu AR, Jones EY, Davis SJ, Dwek RA, Rudd PM. 2006. Inhibition of hybrid- and complex-type glycosylation reveals the presence of the GlcNAc transferase I-independent fucosylation pathway. Glycobiology. 16:748–756.

Ferrara C, Brunker P, Suter T, Moser S, Puntener U, Umana P. 2006. Modulation of therapeutic antibody effector functions by glycosylation engineering: influence of Golgi enzyme localization domain and co-expression of heterologous β1,4-*N*-acetylglucosaminyltransferase III and Golgi α-mannosidase II. Biotechnol Bioeng. 93:851–861.

Ferrara C, Stuart F, Sondermann P, Brunker P, Umana P. 2006. The carbohydrate at FcγRIIIa Asn-162. An element required for high affinity

binding to non-fucosylated IgG glycoforms. J Biol Chem. 281: 5032–5036.

Harada H, Kamei M, Tokumoto Y, Yui S, Koyama F, Kochibe N, Endo T, Kobata A. 1987. Systematic fractionation of oligosaccharides of human immunoglobulin G by serial affinity chromatography on immobilized lectin columns. Anal Biochem. 164:374–381.

Harris LJ, Skaletsky E, Mcpherson A. 1998. Crystallographic structure of an intact IgG1 monoclonal antibody. J Mol Biol. 275:861–872.

Huber R, Deisenhofer J, Colman PM. 1976. Crystallographic structure studies of an IgG molecule and an Fc fragment. Nature. 264:415–420.

Iida S, Misaka H, Inoue M, Shibata M, Nakano R, Yamane-Ohnuki N, Wakitani M, Yano K, Shitara K, Satoh M. 2006. Non-fucosylated therapeutic IgG1 antibody can evade the inhibitory effect of serum immunoglobulin G on antibody-dependent cellular cytotoxicity through its high binding to FcγRIIIa. Clin Cancer Res. 12:2879–2887.

Jefferis R. 2002. Glycosylation of human IgG antibodies: relevance to therapeutic applications. BioPharm. 14:19–26.

Jefferis R. 2005. Glycosylation of recombinant antibody therapeutics. Biotechnol Prog. 21:11–16.

Jefferis R, Lund J. 2002. Interaction sites on human IgG-Fc for FcγR: current models. Immunol Lett. 82:57–65.

Jefferis R, Lund J, Pound J. 1998. IgG-Fc mediated effector functions: molecular definition of interaction sites for effector ligands and the role of glycosylation. Immunol Rev. 163:59–76.

Junghans RP, Anderson CL. 1996. The protection receptor for IgG catabolism is the β2-microglobulin-containing neonatal intestinal transport receptor. Proc Natl Acad Sci USA. 93:5512–5516.

Kamoda S, Nomura C, Kinoshita M, Nishiura S, Ishikawa R, Kakehi K, Kawasaki N, Hayakawa T. 2004. Profiling analysis of oligosaccharides in antibody pharmaceuticals by capillary electrophoresis. J Chromatogr A. 1050:211–216.

Kanda Y, Yamane-Ohnuki N, Sakai N, Yamano K, Nakano R, Inoue M, Misaka H, Iida S, Wakitani M, Konno Y et al. 2006. Comparison of cell lines for stable production of fucose-negative antibodies with enhanced ADCC. Biotechnol Bioeng. 94:680–688.

Lin AI, Philipsberg GA, Haltiwanger RS. 1994. Core fucosylation of high-mannose-type oligosaccharides in GlcNAc transferase I-deficient (Lec1) CHO cells. Glycobiology. 4:895–901.

Malaise MG, Hoyoux C, Franchimont P, Mahieu PR. 1990. Evidence for a role of accessible galactosyl or mannosyl residues of Fc domain in the *in vivo* clearance of IgG antibody-coated autologous erythrocytes in the rat. Clin Immunol Immunopathol. 54:469–483.

Mizuochi T, Taniguchi T, Shimizu A. 1982. Structural and numerical variations of the carbohydrate moiety of immunoglobulin G. J Immunol. 129: 2016–2020.

Mori K, Kuni-Kamochi R, Yamane-Ohnuki N, Wakitani M, Yamano K, Imai H, Kanda Y, Niwa R, Iida S, Uchida K et al. 2004. Engineering Chinese hamster ovary cells to maximize effector function of produced antibodies using *FUT8* siRNA. Biotechnol Bioeng. 88:901–908.

Nakamura K, Tanaka Y, Fujino I, Hirayama N, Shitara K, Hanai N. 2000. Dissection and optimization of immune effector functions of humanized anti-ganglioside GM2 monoclonal antibody. Mol Immunol. 37: 1035–1046.

Natsume A, Wakitani M, Yamane-Ohnuki N, Shoji-Hosaka E, Niwa R, Uchida K, Satoh M, Shitara K. 2005. Fucose removal from complex-type oligosaccharide enhances the antibody-dependent cellular cytotoxicity of single-gene-encoded antibody comprising a single-chain antibody linked the antibody constant region. J Immunol Methods. 306:93–103.

Niwa R, Hatanaka S, Shoji-Hosaka E, Sakurada M, Kobayashi Y, Uehara A, Yokoi H, Nakamura K, Shitara K. 2004. Enhancement of the antibody-dependent cellular cytotoxicity of low-fucose IgG1 is independent of FcγRIIIa functional polymorphism. Clin Cancer Res. 10:6248–6255.

Niwa R, Natsume A, Uehara A, Wakitani M, Iida S, Uchida K, Satoh M, Shitara K. 2005. IgG subclass-independent improvement of antibody-dependent cellular cytotoxicity by fucose removal from Asn297-linked oligosaccharides. J Immunol Methods. 306:151–160.

Niwa R, Sakurada M, Kobayashi Y, Uehara A, Matsushima K, Ueda R, Nakamura K, Shitara K. 2005. Enhanced natural killer cell binding and activation by low-fucose IgG1 antibody results in potent antibody-dependent cellular cytotoxicity induction at lower antigen density. Clin Cancer Res. 11:2327–2336.

Niwa R, Shoji-Hosaka E, Sakurada M, Shinkawa T, Uchida K, Nakamura K, Matsushima K, Ueda R, Hanai N, Shitara K. 2004. Defucosylated anti-CC chemokine receptor 4 IgG1 with enhanced antibody-dependent cellular cytotoxicity shows potent therapeutic activity to T cell leukemia and lymphoma. Cancer Res. 64:2127–2133.

Nose M, Heyman B. 1990. Inhibition of processing of asparagine-linked carbohydrate chains on IgG2a by using swainsonine has no influence upon antibody effector functions *in vitro*. J Immunol. 145:910–914.

Ober J, Martinez C, Lai X, Zhou J, Ward S. 2004. Exocytosis of IgG as mediated by the receptor, FcRn: an analysis at the single-molecule level. Proc Natl Acad Sci USA. 101:11076–11081.

Ohta S, Honda A, Tokutake Y, Yoshida H, Hanai N. 1993. Antitumor effects of a novel monoclonal antibody with high binding affinity to ganglioside GD3. Cancer Immunol Immunother. 36:260–266.

Okazaki A, Shoji-Hosaka E, Nakamura K, Wakitani M, Uchida K, Kakita S, Tsumoto K, Kumagai I, Shitara K. 2004. Fucose depletion from human IgG1 oligosaccharide enhances binding enthalpy and association rate between IgG1 and FcγRIIIa. J Mol Biol. 336:1239–1249.

Papac I, Briggs B, Chin T, Jones J. 1998. A high-throughput microscale method to release *N*-linked oligosaccharides from glycoproteins for matrix-assisted laser desorption/ionization time-of-flight mass spectrometric analysis. Glycobiology. 8:445–454.

Radaev S, Motyka S, Fridman WH, Sautes-Fridman C, Sun PD. 2001. The structure of a human type III Fcgamma receptor in complex with Fc. J Biol Chem. 276:16469–16477.

Rademacher TW, Parekh RB, Dwek RA. 1988. Glycobiology. Annu Rev Biochem. 57:785–838.

Ripka J, Adamany A, Stanley P. 1986. Two Chinese hamster ovary glycosylation mutants affected in the conversion of GDP-mannose to GDP-fucose. Arch Biochem Biophys. 249:533–545.

Rothman J, Perussia B, Herlyn D, Warren L. 1989. Antibody-dependent cytotoxicity mediated by natural killer cells is enhanced by castanospermine-induced alterations of IgG glycosylation. Mol Immunol. 26:1113–1123.

Schenerman MA, Hope JN, Kletke C, Singh JK, Kimura R, Tsao EI, Folena-Wasserman G. 1999. Comparability testing of a humanized monoclonal antibody (synagis) to support cell line stability, process validation, and scale-up for manufacturing. Biologicals. 27:203–215.

Schuster M, Umana P, Ferrara C, Brunker P, Gerdes C, Waxenecker G, Wiederkum S, Schwager C, Loibner H, Himmler G et al. 2005. Improved effector functions of a therapeutic monoclonal Lewis Y-specific antibody by glycoform engineering. Cancer Res. 65:7934–7941.

Shields RL, Lai J, Keck R, O'Connell LY, Hong K, Meng YG, Weikert SH, Presta LG. 2002. Lack of fucose on human IgG1 *N*-linked oligosaccharide improves binding to human FcγRIII and antibody-dependent cellular toxicity. J Biol Chem. 277:26733–26740.

Shinkawa T, Nakamura K, Yamane N, Shoji-Hosaka E, Kanda Y, Sakurada M, Uchida K, Anazawa H, Satoh M, Yamasaki M et al. 2003. The absence of fucose but not the presence of galactose or bisecting *N*-acetylglucosamine of human IgG1 complex-type oligosaccharides shows the critical role of enhancing antibody-dependent cellular cytotoxicity. J Biol Chem. 278:3466–3473.

Stanley P, Chaney W. 1985. Control of carbohydrate processing: the lec1A CHO mutation results in partial loss of *N*-acetylglucosaminyltransferase I activity. Mol Cell Biol. 5:1204–1211.

Tao MH, Smith RI, Morrison SL. 1993. Structural features of human immunoglobulin G that determine isotype-specific differences in complement activation. J Exp Med. 178:661–667.

Thornburg RW, Day JF, Baynes JW, Thorpe SR. 1980. Carbohydrate-mediated clearance of immune complexes from the circulation. A role for galactose residues in the hepatic uptake of IgG-antigen complexes. J Biol Chem. 255:6820–6825.

Uozumi N, Yanagidani S, Miyoshi E, Ihara Y, Sakuma T, Gao CX, Teshima T, Fujii S, Shiba T, Taniguchi N. 1996. Purification and cDNA cloning of porcine brain GDP-L-Fuc:*N*-acetyl-β-D-glucosaminide α1,6-fucosyltransferase. J Biol Chem. 271:27810–27817.

Urlaub G, Chasin LA. 1980. Isolation of Chinese hamster cell mutants deficient in dihydrofolate reductase activity. Proc Natl Acad Sci USA. 77: 4216–4220.

Wright A, Morrison SL. 1994. Effect of altered C_H2-associated carbohydrate structure on the functional properties and *in vivo* fate of chimeric mouse-human immunoglobulin G1. J Exp Med. 180:1087–1096.

Wright A, Morrison SL. 1998. Effect of C2-associated carbohydrate structure on Ig effector function: studies with chimeric mouse-human IgG1 antibodies in glycosylation mutants of Chinese hamster ovary cells. J Immunol. 160:3393–3402.

Wright A, Sato Y, Okada T, Chang K, Endo T, Morrison S. 2000. *In vivo* trafficking and catabolism of IgG1 antibodies with Fc associated carbohydrates of differing structure. Glycobiology. 10:1347–1355.

Yamane-Ohnuki N, Kinoshita S, Inoue-Urakubo M, Kusunoki M, Iida S, Nakano R, Wakitani M, Niwa R, Sakurada M, Uchida K et al. 2004. Establishment of *FUT8* knockout Chinese hamster ovary cells: an ideal host cell line for producing completely defucosylated antibodies with enhanced antibody-dependent cellular cytotoxicity. Biotechnol Bioeng. 87:614–622.

Yanagidani S, Uozumi N, Ihara Y, Miyoshi E, Yamaguchi N, Taniguchi N. 1997. Purification and cDNA cloning of GDP-L-Fuc:*N*-acetyl-beta-D-glucosaminide: alpha1–6 fucosyltransferase (alpha1–6 FucT) from human gastric cancer MKN45 cells. J Biochem (Tokyo). 121: 626–632.